Desalination and Water Treatment
www.deswater.com
doi: 10.5004/dwt.2021.26704

214 (2021) 321–337
February

A detailed analysis of the influence of selected process parameters on the desalination of geothermal water using nanofiltration/reverse osmosis membranes

M. Tyszer[a,b,*], B. Tomaszewska[a,*]

[a]*AGH - University of Science and Technology, Faculty of Geology, Geophysics and Environmental Protection, Department of Fossil Fuels, Mickiewicza 30 Av., 30-059 Kraków, Poland, emails: magdatyszer@gmail.com/mtyszer@meeri.com (M. Tyszer), barbara.tomaszewska@agh.edu.pl (B. Tomaszewska)*
[b]*Mineral and Energy Economy Research Institute Polish Academy of Science, Wybickiego Street 7A, 31-261 Krakow, Poland*

Received 5 May 2020; Accepted 20 August 2020

ABSTRACT

Natural geothermal water, which often possesses high levels of total dissolved solids, can be desalinated or concentrated by different membrane processes with different efficiency ratios. The paper presents the results of an assay designed to examine the potential relationship between the membrane process and water composition parameters and the efficiency of the water concentration system. In the research presented in this paper, different process parameters were investigated: various membrane processes, types of apparatus, values of permeate recovery, transmembrane pressures, commercially available membrane types, selected antiscalants and feed water temperatures. The results of the study demonstrate that a proper selection of the process parameters can produce a significant increase in the values of absolute and average permeate flux and consequently increase the efficiency of the process and decrease energy demand. Recommended values of desalination process parameters were proposed for individual waters based on the results of the research and taking into account the type of apparatus used during laboratory tests. For medium- and highly mineralised waters, higher transmembrane pressure values, lower permeate recovery rates and more-compacted membranes were recommended than for lightly mineralised waters.

Keywords: Desalination; Unit efficiency; Geothermal water; Nanofiltration; Reverse osmosis; Water management

1. Introduction

In recent years, the widely understood efficiency of processes or technological solutions is a key factor in the development of many branches of industry, including renewable energy sources. Nowadays, efficiency is an important aspect of every action, and it is also an important factor for such high-energy operations as membrane processes, especially for reverse osmosis (RO) and nanofiltration (NF). Both membrane processes mentioned are widely applied in the desalination of seawater and geothermal waters, the production of drinking water, and recently also in tertiary wastewater treatment [1]. The processes face a number of challenges consequent on the ever-increasing demand for efficiency in parallel with environmentally friendly management of products thus obtained (permeates and retentates) [2,3].

RO processes have recently become one of the most widely used seawater, wastewater or geothermal water desalination and treatment technologies worldwide [4]. Moreover, more than 60% of the desalination plants in operation use membrane technology, primarily RO, because of

* Corresponding authors.

its reliability [5]. Unfortunately, the relatively high energy consumption of RO compared with other processes leads scientists to seek novel membrane materials, improved apparatus design, and increased process efficiency [6], and to analyse the possibility of combining it with other processes [7] and also to carry out tests to optimise the quantity and quality of water production and the processes involved to further reduce the specific energy consumption [8], and consequently the cost of water desalination [9]. For membrane-based technologies, the amount of energy demand can be reduced by combining different processes (solar energy) and methods (NF-RO), producing more profitable membranes [10], using more effective pumps, or by adjusting the relevant values of the process parameters [11].

Apart from the technological aspects, geothermal waters present specific physical and chemical compositions, often exhibiting high concentrations of silica, sulphates, calcium, magnesium, strontium, barium and carbonate, which may affect the useful life of the membrane, decrease efficiency during desalination [12] or the concentration of water using membrane processes, limit the flux recovery and increase the operating costs [13].

The production and treatment of water require energy, the quantity of which can vary considerably depending on the process and technology used. In general, thermal processes require more energy [14] than membrane-based processes, including RO or NF. Energy optimisation of desalination processes, primarily RO, has led to significant reductions in energy consumption, mostly through membrane developments, improvements in pump efficiency and the optimisation of permeate flux [8]. The scaling phenomenon, which can occur, is a complex process involving the crystallisation or precipitation of minerals [14], so it is a very important aspect, which it is essential to consider. The saturation limit is the concentration of specific ions in the solution above which crystallisation or precipitation of calcium carbonate (aragonite, calcite), calcium sulphate (anhydrite, gypsum), barium sulphate (barite), strontium sulphate (celestite), silicates (chalcedony, silica) or calcium phosphate (apatite, hydroxyapatite) become thermodynamically possible. Membrane scaling directly affects the efficiency of the process being carried out by a significant decline in permeate flux [15]. The probability of scale formation also increases due to the concentration of polarisation. This is defined as the concentration gradient of salts developed in the vicinity of the membrane surface due to the redilution of the salts remaining as water permeates through the membrane itself. However, high permeate fluxes and low cross-flow velocities may further enhance the concentration gradient between the surface and the bulk fluid through the concentration polarisation phenomenon (which does not solely depend on the operating conditions) [16,17]. To avoid this problem, the feed water is normally dosed with antiscalants during the membrane process [18,19]. Scientists from all over the world have conducted numerous pieces of research devoted to increasing the efficiency of the NF or RO processes and have demonstrated that by optimising the process parameters [20], using unconventional sources of energy [11,21], improving membranes [22,23] and the efficiency with which permeate flux is regulated [24,25], the performance of a desalination plant may be improved [26] and simultaneously the cost may be reduced [27].

The results of selective laboratory tests related to the treatment of geothermal waters have been presented in a partial version in some of the authors' works [2,3,28–33], but the aim of this work is to analyse the influence of the whole range of process parameters which determine the results on a detailed analysis. That is why this paper presents an integrated multi-factor analysis based on the results of a complex research programme simulating the membrane processes on selected geothermal waters through the specification of different process parameters. The research was designed to examine the influence of selected parameters such as: (1) type of membrane process (NF and RO), (2) apparatus type (cross-flow or dead-end mode), (3) level of permeate recovery (50% and 75%), (4) value of transmembrane pressure (TP) (10 bar for NF and 15 bar for RO), (5) membrane type (two NF and four RO membranes), (6) addition of antiscalant and (7) feed water temperature (15°C, 22°C and 30°C) on the unit efficiency of the NF/RO desalination system in concentrating geothermal water. The research included all steps of the analysis, from laboratory tests on selected waters to comparative analysis of the changes of absolute and average permeate flux during the processes conducted with different process parameter settings. The purpose of the assay was to examine whether there is a correlation between the parameters selected (type of membrane, addition of antiscalant, pressure, temperature) and the actual unit efficiency (variation in permeate flux) in the concentration of geothermal water, as a solution to obtaining new products, useful in cosmetology, balneology and other fields.

2. Materials and methods

2.1. Geothermal waters

The tests were conducted on the basis of three geothermal waters marked as MM (medium mineralised), HM (highly mineralised) and LM (lightly mineralised). All waters selected for testing were obtained from wells located in central and southern Poland. The first MM geothermal water, in its natural state, has a mineralisation of more than 2.4 g/L, a high concentration of metasilicic acid (more than 79 mg/L) and a relatively high concentration of other components such as: magnesium (more than 41 mg/L), calcium (more than 194 mg/L) and other micro and macro elements. The highest concentrations were determined for sulphates (854 mg/L), chlorides (487 mg/L), sodium (488 mg/L) and calcium (194 mg/L) in the physicochemical composition of the water studied, which according to the classification of Szczukariew-Prikłoński, gives the water the SO_4–Cl–Na–Ca hydrogeochemical type. The second HM geothermal water is more highly mineralised (6.7 mg/L) having an increased content of metasilicic acid (34 mg/L), calcium (127 mg/L) and magnesium (21 mg/L). The hydrogeochemical type of this water is Na–Cl. On the other hand, the third LM geothermal water, in its natural state, has a low total mineralisation (0.5 g/L) and increased content of specific components: iron ions (0.32 mg/L) and metasilicic acid (26.57 mg/L). The ionic composition is dominated by bicarbonates (319.2 mg/L), calcium (58.69 mg/L)

and sodium (34.71 mg/L), giving the water the HCO_3–Ca–Na hydrogeochemical type. The water composition was determined in an accredited laboratory in accordance with international standards with the use of inductively coupled plasma mass spectrometry (ICP-MS), inductive coupled plasma optical emission spectrometry (ICP-OES) and the titration method. Detailed hydrogeochemical characteristics of the raw geothermal waters are presented in Table 1.

2.2. Apparatus

All the tests were carried out on a laboratory scale with the use of two different sets of apparatus. The first apparatus used was for the dead-end mode – a one-step desalination system consisting of a stirred cell device in a high-pressure version (Fig. 1). For the NF and RO processes the raw geothermal water was placed in a stirred cell under the prescribed pressure. During all tests conducted the feed water was passed to the membrane and concentrate was retained in the stirred cell in the membrane. The NF and RO tests were carried out to obtain 50% and 75% permeate recovery. The active area of each membrane was 38 cm^2 [28–30]. The second apparatus used was the American Osmonics Inc., (5951 Clearwater Drive, Minnetonka, Minnesota, USA). Company's SEPA CF-HP type membrane module (Fig. 2). The active area of the particular NF and RO membrane was 155 cm^2. The feed water was placed in a tank from which a water stream was pumped through a high-pressure pump to the membrane cavity of the module. Then, from the cavity the stream of

Table 1
Physicochemical characteristics of geothermal waters used in research

Parameter	Raw MM (mg/L)	Raw HM (mg/L)	Raw LM (mg/L)
Na^+	488.7	2,417.0	34.71
K^+	47.6	20.5	15.2
Li^+	1.138	0.174	0.019
Be^{+2}	0.0005	0.0005	0.0005
Ca^{+2}	194.1	127.8	58.69
Mg^{+2}	41.6	21.5	13.5
Ba^{+2}	0.0436	0.0921	0.0184
Sr^{+2}	6.244	4.947	1.079
Fe^{+2}	0.232	0.498	0.323
Mn^{+2}	0.005	0.038	0.012
Ag^+	0.001	0.001	0.002
Zn^{+2}	0.010	0.111	0.010
Cu^{+2}	0.002	0.025	0.001
Co^{+2}	0.0011	0.0004	0.0002
Se^{+2}	0.010	0.010	0.010
Sb^{+3}	0.0004	0.0002	0.0002
Mo^{+6}	0.0759	0.0013	0.0003
V^{+5}	0.004	0.014	0.001
Zr^{+4}	0.002	0.002	0.005
Ti^{+4}	0.074	0.020	0.020
As^{+3}	0.002	0.007	0.001
Tl^{+4}	0.0001	0.0001	0.0001
W^{+6}	0.0293	0.0003	0.0003
Cl^-	487.9	3,719.0	16.5
Br^-	0.769	1.383	0.100
I^-	0.099	0.053	0.010
SO_4^{-2}	854.7	72.34	4.13
HCO_3^-	343.3	273.8	319.2
CO_3^{-2}	0.500	0.500	0.500
PO_4^{-3}	1.5339	0.0061	0.4290
BO_3^{-3}	53.115	5.181	0.463
HBO_2	39.571	3.860	0.345
H_2SiO_3	79.43	34.01	26.57
Mineralisation	2,416.10	6,697.80	491.4
Total hardness (mg$CaCO_3$/L)	655.4	407.6	202.1

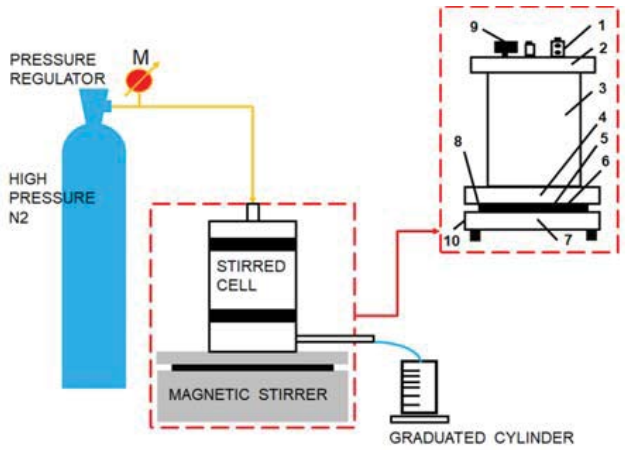

Fig. 1. Scheme of apparatus used in NF/RO processes, in dead-end version (1 – safety valve; 2 – top cover; 3 – pressure cylinder; 4 – magnetic stirrer; 5 – membrane; 6 – perforated plate; 7 – lower cover; 8 – gasket; 9 – gas supply; 10 – permeate discharge) (based on the study by Tyszer and Tomaszewska [30]).

water flows tangentially across the membrane surface. Part of the feed water permeates through the membrane and flows to the permeate carrier, which is placed on the top part of the membrane cavity and flows out through the permeate outlet into a graduated vessel. The part of the feed water which does not flow through the membrane, the concentrate, continues sweeping over the membrane surface and collects in the multiplier. The concentrate flows through the concentrate flux control valve and recirculates to the feed tank [31–33]. Each NF and RO membrane was conditioned by the filtration of deionised water before the main test to check the efficiency of particular membranes and to gain the value of the deionised water permeate flux.

2.3. Selected process parameters

All the tests were carried out at an almost constant temperature of 22°C for RO processes and 15°C and 30°C for NF. The value of the temperature was stabilised by applying a heat exchanger and was measured with an accuracy ±0.5°C. For the tests conducted with the use of the apparatus presented in Fig. 1, the amount of feed water was 300 mL and for the second apparatus (Fig. 2) was 5,000 mL. The processes were carried out at a specified TP of 10 bar for NF and 15 bar for RO (osmotic pressure was not taken into consideration). A single attempt was conducted for each experiment (there were no repeats).

2.4. Membranes

Based on a preliminary theoretical analysis, four commercially available RO membrane types were selected for testing:

- DOW FILMTEC™BW30FR-400 (Dow Water & Process Solutions Company, 600 Metro Blvd, Minneapolis, Minnesota, USA) - BW30FR;
- DOW FILMTEC™BW30HR-440i (Dow Water & Process Solutions Company, 600 Metro Blvd, Minneapolis, Minnesota, USA) - BW30HRi;
- AG Membrane (GE Power Water & Process Technologies Company, 5 Necco Street, Boston, Massachusetts, USA) - AG;
- LEWABRANE®RO B400 HR (LANXESS Energizing Chemistry Company, Kennedyplatz 1, Cologne, Germany) - BWHR,

and two types of NF membranes:

- DOW FILMTEC™NF270 (Dow Water & Process Solutions Company, 600 Metro Blvd, Minneapolis, Minnesota, USA) - NF-LC;
- DOW FILMTEC™NF90 (Dow Water & Process Solutions Company, 600 Metro Blvd, Minneapolis, Minnesota, USA) - NF-MC.

The RO membranes selected are designed for use in brackish water treatment systems and are characterised by a high retention factor of the undesirable components contained in desalinated water and a resistance to scaling phenomena. The BW30FR membrane is designed for the purification of water with a high content of biological or organic impurities. Its properties also include a

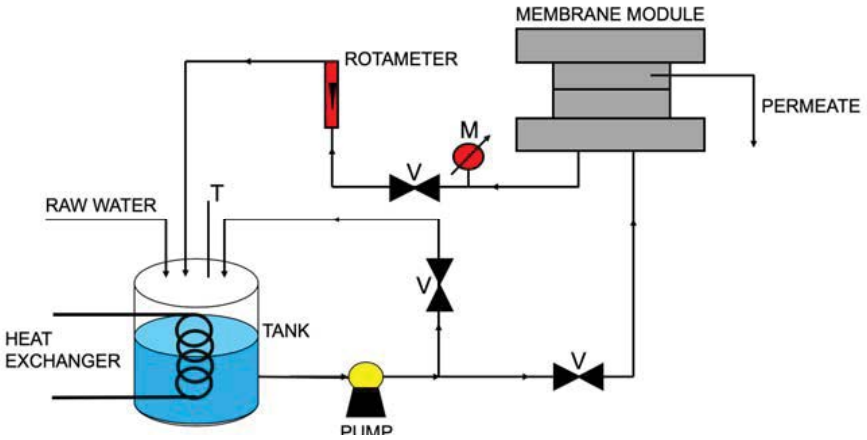

Fig. 2. Diagram of apparatus used in nanofiltration/reverse osmosis processes with a CF-HP membrane module, in high-pressure cross-flow version (based on the study by Tomaszewska et al. [33]).

high retention coefficient of compounds contained in the water, a high efficiency over a long period of use, exceptionally high resistance to fouling and being easy to clean [34]. The BW30HRi membrane is also described as a very high-performance product combined with the largest active surface of the membrane currently available in the market for the treatment of brackish water. In accordance with the manufacturer's declaration [35], it is possible to obtain a high-quality permeate with this membrane without increasing the volume of the permeate stream. The BWHR membrane is designed for the industrial treatment of water of both low and high salinity. It is a thin film composite polyamide membrane, with a salt retention factor of approximately 99.7% [36]. On the other hand, the AG membrane is characterised by a high level of sodium chloride retention and resistance to high volumes of permeate stream. It is recommended for the effective reduction of salinity and the reduction of some ingredients [37]. The NF membranes used in the study were thin film composite polyamide membranes, characterised by over 98% retention of $MgSO_4$. The NF-LC membrane, which enables a 50% transfer of salt to the permeate solution with a slight reduction in water hardness, is used in cases where it is desirable to remove organic impurities with partial water softening [38]. NF-MC provides high performance with high (90%–96%) removal of salts, nitrates, iron and organic compounds [39]. A detailed comparison of these four membranes is presented in Table 2.

The NF-LC membranes are less-compacted with separation than DOW NF-MC membranes. BW30FR membranes have high productivity fouling resistant elements, and are designed for waters with high fouling potential, allowing the operator to maximise the process efficiency [36]. The BW30HRi membranes were created to ensure better effects when treating brackish waters by increasing productivity and rejection. Moreover, these membranes were additionally enriched with i-LEC™ technology to reduce the system operating cost and the risk of o-ring leaks that can cause decreased permeate water quality. Compared with BW30FR, these membranes provide significantly higher boron rejection [37]. AG membranes provide a high flux rate and high sodium chloride rejection with a relatively low operating pressure [39]. The main difference between BW30HRi and BWHR membranes is the intended use of the membranes. BWHR are designed for the industrial treatment of brackish and low salinity waters, whereas BW30HRi membranes, due to their special i-LEC™ technology, provide visibly higher productivity and rejection (including the boron ion).

2.5. Antiscalants

Five widely available antiscalants (Table 3) were selected to prevent the formation of secondary sediments on the membrane surface, primarily carbonate, silica and aluminosilicate, to be used in chemical scale-reduction tests. For antiscalant tests, a pre-determined dosage of the substance was added to the raw water before the feed was placed in the feed tank. The dose was adjusted so that the pH value of the geothermal water examined did not drop below 5.5 ± 0.5 after the addition of the chemical. The dose for the antiscalants A1 [40] and A2 [41] was set at 1 mL/L, while for the antiscalants A3 [42] and A4 [43] the dose was set at 0.7 mL/L. For A5 [44], doses of 6, 10 and 12 mL/L were applied. The selected chemicals are mixtures of phosphonates and dispersants that are effective in preventing the deposition of sulphates, silica and carbonates on the membrane surface (Table 3) [31].

2.6. Method of calculation of unit efficiency

Before research, each new membrane was conditioned by the filtration of deionised water to stabilise the permeate flux. During the RO tests, with apparatus in the dead-end version, measurements were made of the time needed to obtain each 5 mL of permeate. On the other hand, during all the NF tests conducted with the apparatus in cross-flow version, the cross-flow velocity was maintained at 1 m/s and measurements were made of the time needed to obtain each 50 ml of permeate. The performance of the desalination process was determined by measuring the changes in absolute and average permeate flux J_v:

$$J_v = \frac{V}{(F \cdot t)} \tag{1}$$

where: V – volume of permeate (L), F – active area of the membrane (m^2), f – filtration time (h).

3. Results and discussion

The results of the research conducted in relation to the selected process parameters and geothermal waters are shown in Figs. 3–12. In this study, three geothermal waters with different mineralisation characteristics were employed (Table 1). For all NF and RO tests, permeability was calculated using permeate flow rates and effective membrane area. Figs. 3–12 show the changes in absolute permeate flux (J_v) with time during all the NF and RO processes of the geothermal waters tested. These changes were analysed in relation to a particular set process parameters.

3.1. Two types of membrane processes (NF and RO)

Research was undertaken on the impact of membrane process (NF and RO) on the relative and average permeate flux (unit efficiency). According to established process properties, the NF and RO processes were conducted with the following parameters: (1) MM and HM, (2) 50% recovery of permeate, (3) TP 10 and 15 bar, (4) NF-LC and BW30FR membranes, (5) temperature 22°C, and (6) apparatus in cross-flow mode. As can be seen, the results indicated (Fig. 3) that with the passage of operating time the permeability was quite stable in all cases, but the efficiency slightly decreases. The lowest value of absolute permeate flux was observed for the test with the use of the RO process for HM in which it decreases from 15 to 13 L/m²h. Moreover, the RO process gave an average permeate flux of 14 L/m²h. The highest decrease was established for a test with the NF process for MM, the process took almost 9 h to obtain the required amount of permeate. On the other hand, in this case (NF process with MM), the average permeate flux was slightly lower than for the RO process and amounted 29 L/m²h. The highest average permeate flux was gained for a

Table 2
Membranes basic information [34–39]

Membrane	DOW FILM-TEC™NF270	DOW FILM-TEC™NF90	DOW FILM-TEC™BW30FR-400	DOW FILM-TEC™BW30HR-440i	AG membrane	LEWABRANE®RO B400 HR
Marked as	NF-LC	NF-MC	BW30FR	BW30HRi	AG	BWHR
Main features	Less-compacted with separation	More-compacted with separation	Fouling resistance, high productivity	Increased Boron rejection, i-LEC™ technology	High flux, high rejection, low pressure	For primary demineralization of brackish and low salinity waters
Retention coefficient	>98% $MgSO_4$ 50% NaCl	>98% $MgSO_4$ 90%–96% NaCl	99.65% NaCl	99.7% NaCl	99.5% NaCl	99.7% NaCl
Material	Polyamide thin-film composite	Polyamide thin-film composite	Polyamide thin-film composite	Polyamide thin-film composite	Polyamide thin-film composite	Polyamide thin-film composite
Maximum operating temperature (°C)	45	45	45	45	45	45
pH operating range	2–11	2–11	2–11	2–11	2–11	2–11
Maximum operating pressure (MPa)	4.1	4.1	4.1	4.1	4.1	4.1

Table 3
Characteristics of antiscalants [31,40–44]

Antiscalant	A1	A2	A3	A4	A5
Composition	Liquid formulation based upon a blend phosphonate	Liquid formulation based upon a blend phosphonate	Liquid formulation based upon a blend phosphonate	Liquid formulation based upon a blend phosphonate	Liquid formulation based upon a blend polymeric carboxylic and phosphonic acids
Scale inhibitor	For calcium carbonate and calcium sulphate	For calcium carbonate	For calcium carbonate, calcium sulphate and other mineral scales	For water with high silica content	For water with high silica content
pH of antiscalant	3.3	10–11	1–2	2.5	9.3
Effective against sulphates scale	Yes	Yes	Yes	–	–
Effective against silicates scale	–	–	Yes	Yes	Yes
Effective against carbonates scale	Yes	Yes	Yes	–	Yes

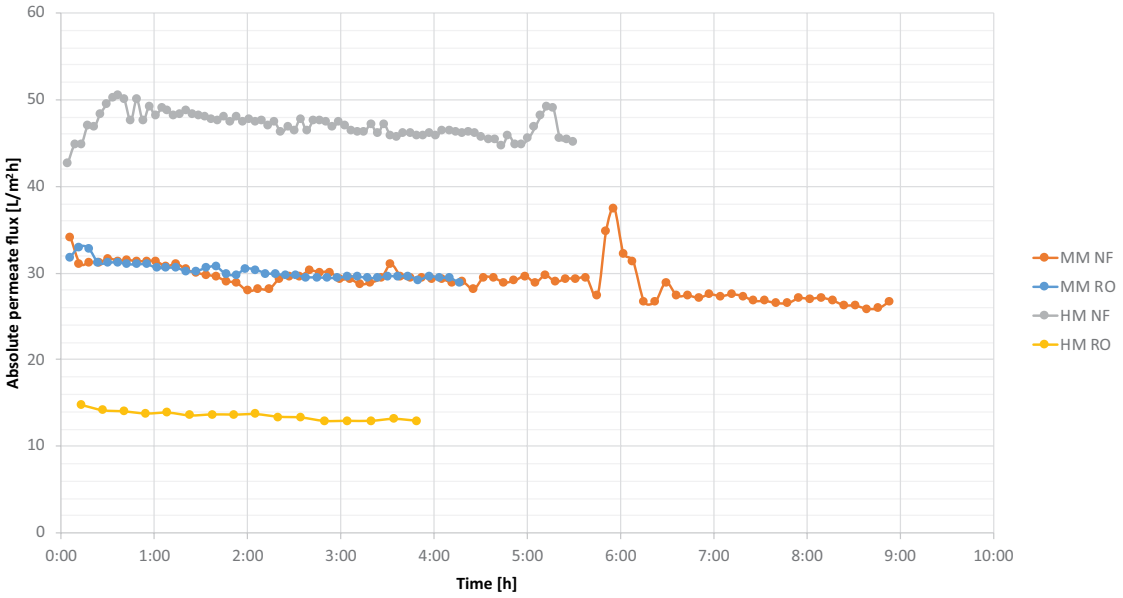

Fig. 3. Comparison changes of absolute permeate flux during two different membrane processes (nanofiltration and reverse osmosis) of medium mineralised and highly mineralized water.

test using NF for HM, 47 L/m²h. The absolute permeate flux oscillates around 30 L/m²h for MM with the RO process, and decreases from 32 to 26 L/m²h for MM with the NF process. A greater apparent difference between the NF and RO processes was observed for HM. The appropriateness of a specific process will be closely linked to the parameters of the raw water, the desired degree of rejection of total dissolved solids and the required process efficiency (energy and economic efficiency). For both MM NF and HM NF, the values of absolute permeate flux suddenly increase above the initial values (after 5 h of operation) probably caused by the sloughing off of secondary minerals from the membrane surface.

3.2. Two apparatus types (cross-flow and dead-end mode)

An investigation was made of the influence of type of apparatus on the average and relative value of permeate flux. The RO process was conducted with the following parameters: (1) MM, HM and LM, (2) 50% recovery of permeate, (3) TP 15 bar, (4) BW30FR membrane, (5) temperature 22°C and (6) apparatus with cross-flow and dead-end mode. Fig. 4 presents experimental data gained from six tests conducted with the use of three different geothermal waters (MM, HM and LM) and two apparatus types. For tests conducted with the use of apparatus in cross-flow mode, the absolute permeate flux remains almost stable with time and oscillated around 30, 23 and 14 L/m²h for MM, LM and HM, respectively. Visible dissimilarity was observed in the case of tests using the dead-end mode apparatus, the tests were carried out with a significant decrease in the value of the absolute permeate flux with time (mostly for MM and HM) from 56, 48 and 29 L/m²h to 51, 39 and 18 L/m²h for LM, MM and HM, respectively. Significantly lower process efficiency in terms of average permeate flux was observed for tests conducted with cross-flow mode apparatus, with rates of 30 L/m²h for MM, 14 L/m²h for HM and 23 L/m²h for LM, compared with processes using dead-end mode apparatus where the rates of flux were 44 L/m²h for MM, 25 L/m²h for HM and 53 L/m²h for LM. In addition, the differences between the types of apparatus used are more pronounced for HM, than for MM and LM, but the same trend of change is visible for all processes. It should be mentioned here that HM water has the highest degree of mineralisation among the waters studied.

3.3. Two values of permeate recovery (50% and 75%)

In this part of the assay, the influence of permeate recovery rate on unit efficiency was investigated. Fig. 5 shows the experimental data of the processes conducted with the use of the following process parameters: (1) MM, HM and LM, (2) 50% and 75% recovery of permeate, (3) TP 15 bar, (4) BW30FR membrane, (5) temperature 22°C and (6) apparatus in dead-end mode. The highest values and lowest decrease of absolute permeate flux with time during the test were established for tests with the use of LM due to the degree of water mineralisation (lowest of all the test waters). The values of relative permeate flux were from 54 to 48 L/m²h (for 50% recovery of permeate) and 54 to 52 L/m²h (for 75% recovery of permeate). The curve shape of the test with LM (50% recovery) indicates that processes were almost stable at the beginning, but absolute permeate flux suddenly increases above the initial values (after 20 min of operation) probably caused by the sloughing off of secondary minerals from the membrane surface. In the case of tests with HM, both processes carried out with the same behaviour, an increase in permeate recovery only deepened the decrease of absolute permeate flux value. A more visible difference between tests was seen in processes using the MM. For the process with 75% recovery of permeate, the absolute permeate flux varied from 44 to only 32 L/m²h. This parameter

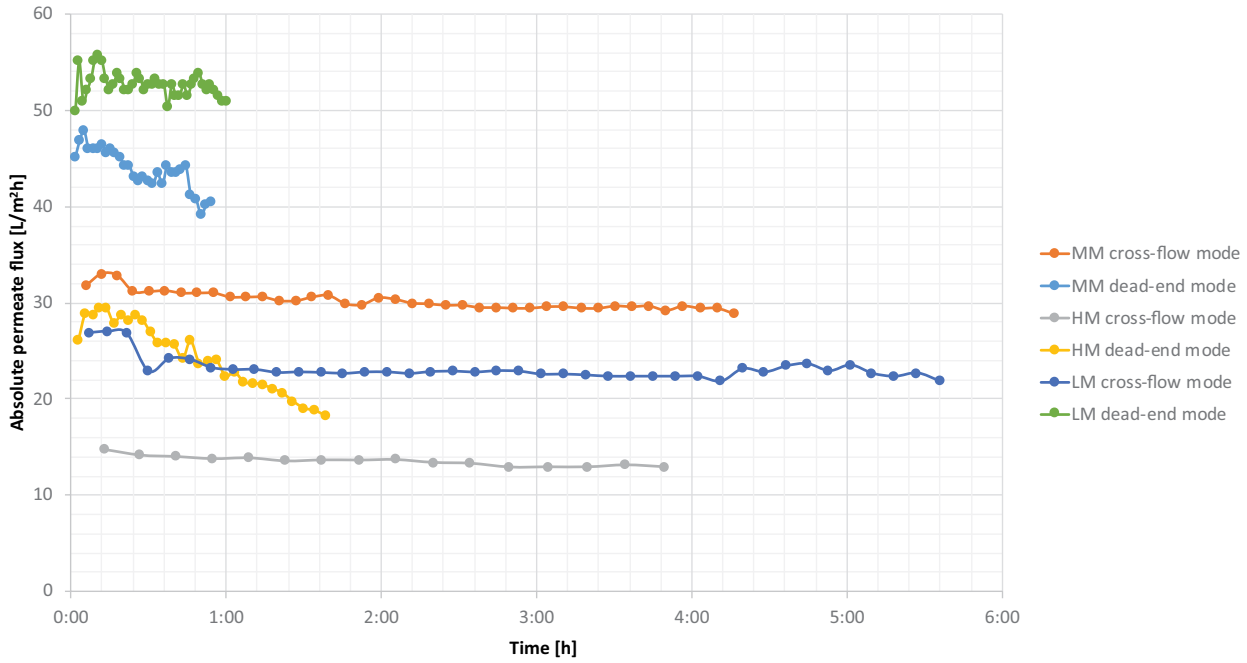

Fig. 4. Comparison changes of absolute permeate flux during reverse osmosis process of medium mineralised, highly mineralised and lightly mineralised water with the use of two different apparatus mode: cross-flow and dead-end.

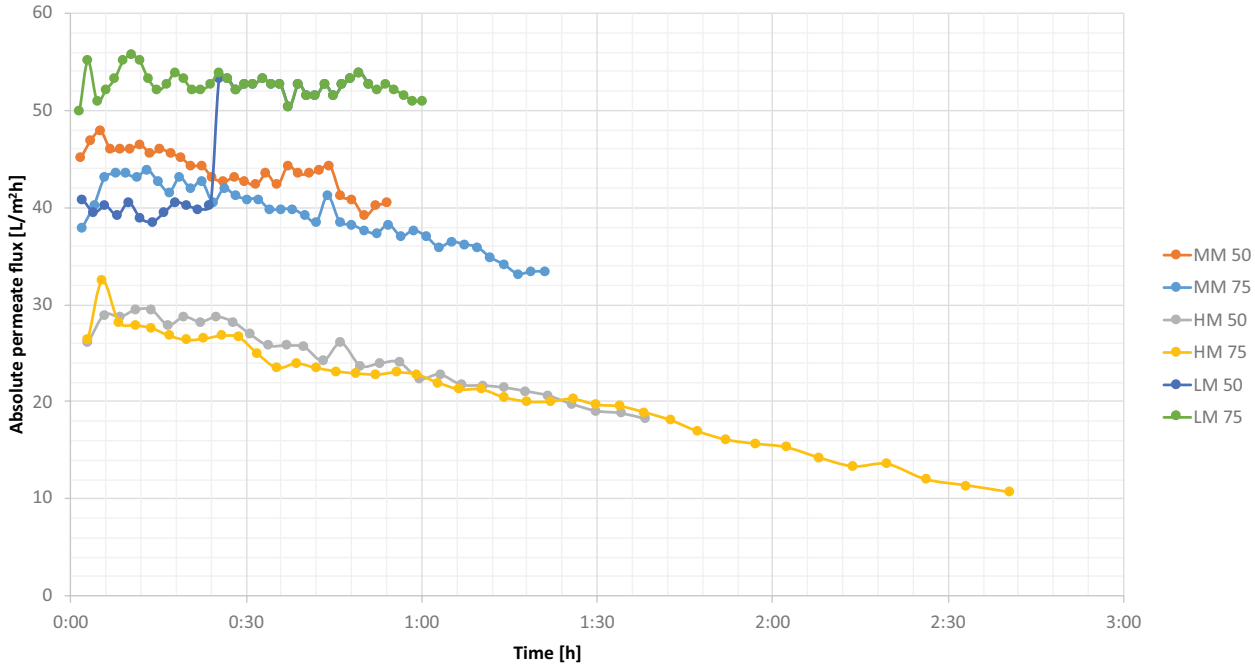

Fig. 5. Comparison changes of absolute permeate flux during reverse osmosis process of medium mineralised, highly mineralised and lightly mineralised water at two different values of permeate recovery (50% and 75%).

changed from 48 to 39 L/m²h for the process with 50% permeate recovery. However, despite this apparent variation, a similar trend of a significant decrease of relative permeate flux with time was observed for both processes. The average permeate flux was 44 L/m²h for MM (50% recovery of permeate), 39 L/m²h for MM (75% recovery of permeate), 25 L/m²h for HM (50% recovery of permeate), 21 L/m²h for HM (75% recovery of permeate), 53 L/m²h for LM (50% recovery of permeate), 47 L/m²h for LM (75% recovery of permeate). The lower value of average permeate flux applies in the case of 75% recovery of permeate. For all cases, an increase in permeate recovery caused an apparent decrease of average

permeate flux (despite LM). On the other hand, for waters with higher mineralisation MM and HM (Table 1), an increase in permeate recovery caused a significant decrease in the absolute permeate flux (in line with the process trend) due to the increasingly serious phenomenon of scaling.

3.4. Two different TPs (10 and 15 bar)

The influence of TP on unit efficiency was tested with the following process parameters: (1) LM, (2) 50% recovery of permeate, (3) TP 10 and 15 bar, (4) BW30FR membrane, (5) temperature 22°C and (6) apparatus with dead-end mode. The data obtained indicates that for feed water with relatively low mineralisation (Table 1, compared with MM and HM), application of a higher TP does not cause a significant increase in unit efficiency. However, as can be seen, values of absolute permeate flux for both processes remain almost stable with time, from 40 L/m²h for 10 bar and 56 L/m²h for 15 bar to 41 and 51 L/m²h, respectively (Fig. 6). This quite significant difference was observed for values of average permeate flux, which were calculated as 39 L/m²h for 10 bar and 53 L/m²h for 15 bar. Generally, a dissimilarity of absolute permeate flux can be caused by a higher rejection of dissolved substances due to increased pressure. Moreover, for waters with higher mineralisation, for example for GT1 and GT2 (Table 1), the difference can be more significant and can increase over time due to the scaling phenomenon.

3.5. Six membrane types (two NF and four RO membranes)

In this part of the study, two NF membranes were tested with the following process parameters being employed: (1) MM and HM, (2) 50% recovery of permeate, (3) TP 10 bar, (4) NF-LC and NF-MC membrane, (5) temperature 22°C and (6) apparatus in cross-flow mode. The data obtained indicates that the absolute permeate flux for the NF-LC membrane, with the use of both MM and HM, produces similar changes with time, in both cases with a slight decrease (Fig. 7). These values oscillate around 32–26 L/m²h for MM and 40–33 L/m²h for GT2. However, the values of average permeate flux differ significantly and are 29 L/m²h for MM (NF-LC membrane) and 34 L/m²h for HM (NF-LC). These results seem to be the opposite to those expected. The specific physicochemical composition of the test waters (content of mono- and bivalent ions) and membrane parameters resulted in higher permeate flux values (with worse component separation) for water with higher mineralisation. One would expect that for water with much higher mineralisation (HM) the absolute and average permeate flux should be lower and the filtration time (until obtaining 50% recovery of permeate) should clearly be longer. This difference may be related to the degree of rejection of individual components in the water, because for water that has a three times greater degree of mineralisation, the duration of the experiment was almost half as long. To obtain higher rejections of selected ions, a more compact NF-MC membrane was applied. In this case, the applicability of the NF-MC membrane also produced results opposite to those expected. Absolute permeate flux clearly increased and varied from 51 to 45 L/m²h, while average permeate flux was 47 L/m²h. This phenomenon is probably caused by the difference in membrane parameters. According to the membrane data sheets, NF-MC provides 10 times higher feed flow rate than NF-LC, while ensuring a higher rejection of ingredients. The sudden increase in the value of absolute permeate flux for MM and HM (after carrying out the

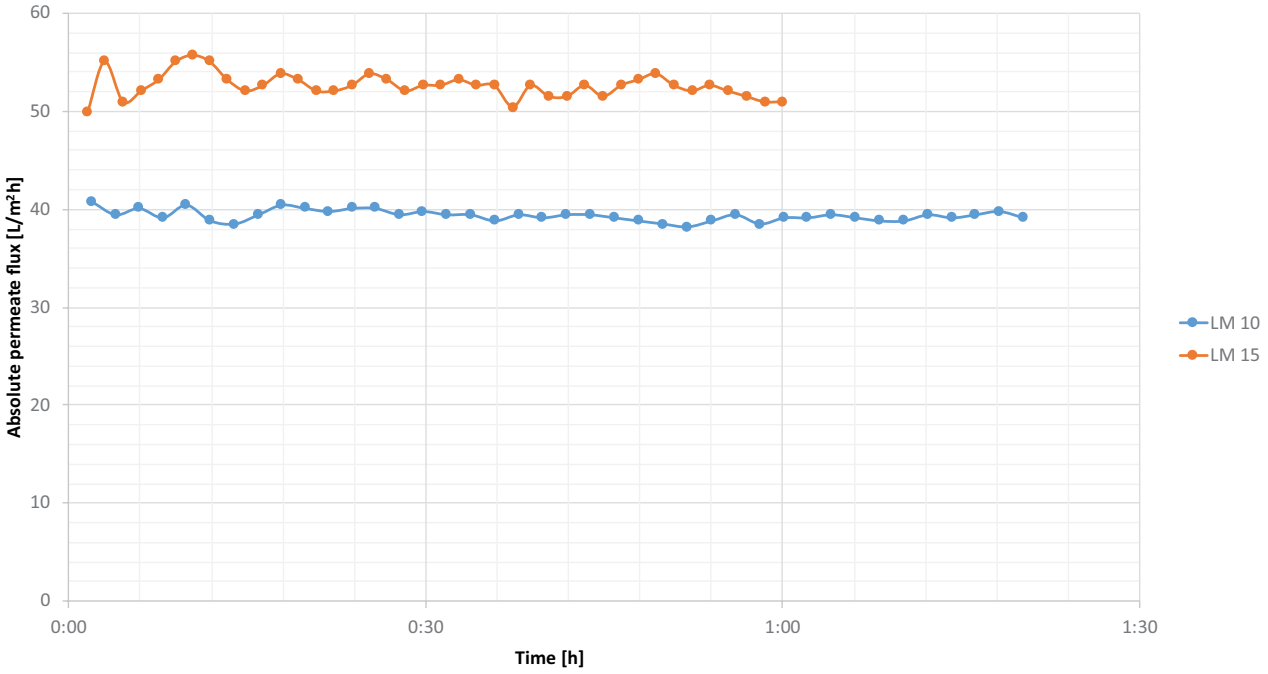

Fig. 6. Comparison changes of absolute permeate flux during membrane processes of lightly mineralised water with the use of two different transmembrane pressure values.

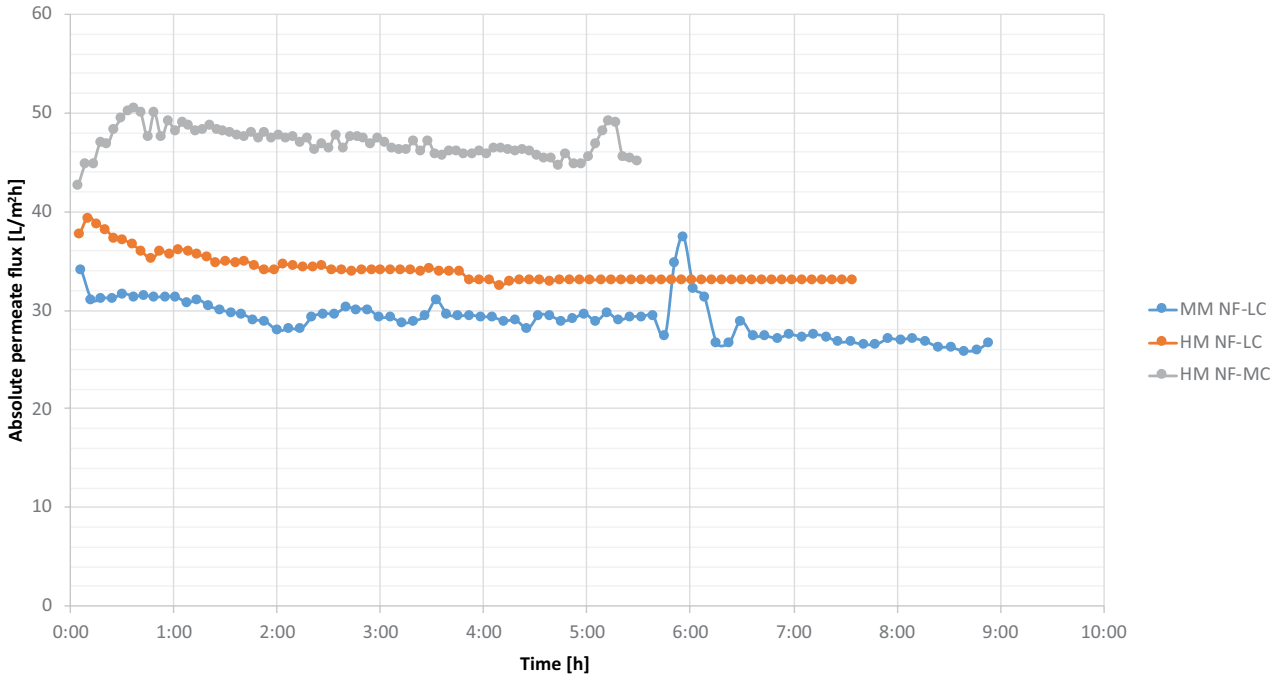

Fig. 7. Comparison changes of permeate flux during nanofiltration (NF) processes of medium mineralised and highly mineralised water with two types of NF membranes.

experiment for 5 h, Fig. 7) can be caused by a similar phenomenon to that mentioned in section 3.1.

The four RO membranes selected for study were tested with the use of the following process parameters: (1) MM and HM, (2) 50% recovery of permeate, (3) TP 15 bar, (4) four different RO membranes, (5) temperature 22°C, (6) apparatus in dead-end mode, which are presented in Fig. 8. For MM the results indicated that in all cases, while the permeability was quite stable with operating time, the efficiency slightly decreases. It showed that the composition of water (Table 1, high silica content and quite high mineralisation) provides favourable conditions so that over a longer timescale scaling phenomenon will indeed be observed, especially for processes with an AG membrane. Despite the highest average permeate flux (53 L/m²h), the highest decrease was established with MM. For the test with the BW30FR membrane, the average permeate flux was 44 L/m²h for MM and 25 L/m²h for HM. As can be seen, the lowest decrease in the value of absolute permeate flux was observed for the process using the BWHR membrane, despite having the lowest values of average permeate flux for both MM and HM water: 25 and 14 L/m²h, respectively. The highest average permeate flux for tests was obtained with the use of the AG membrane, 53 L/m²h for MM. With this membrane the absolute permeate flux oscillates around 58 to 48 L/m²h for the experiment with MM and around 32 to 18 L/m²h for HM. For HM, however, a similar trend was seen. A decrease of permeate flux efficiency with time is more apparent in all the tests, which is similar between BW30FR, BW30HRi and AG membranes. This is related to a higher water mineralisation and the content of scaling-driven ions (Table 1). For tests with HM water and BW30FR, BW30HRi and AG membranes, absolute permeate flux oscillates from around 32 L/m²h to only 18 L/m²h. In the case of MM, for the membranes mentioned, significantly higher process efficiency was observed in terms of absolute permeate flux, with values ranging from 58 to 36 L/m²h, apart from the tests with the AG membrane for both waters. The tests with MM and HM waters and BW30FR membrane were conducted with a visible decrease in absolute permeate flux, however the average permeate flux remained at quite a high level. The application of a fouling resistant membrane seems appropriate for waters with this specific composition (waters susceptible to scaling). The tests with the BW30HRi membrane (which is described as high efficiency with special i-LEC™ technology), were carried out with lower absolute permeate flux values than for the BW30FR (fouling resistant) membrane. In addition, the differences between the membranes used are more pronounced for MM than for HM, but the same trend of change is visible with individual membranes using both waters.

3.6. Five commonly available antiscalants

According to the established properties of the processes, the tests with the addition of antiscalants were carried out using the following parameters for the process: (1) MM (Fig. 9) and HM (Fig. 10), (2) 50% recovery of permeate, (3) TP 15 bar, (4) BW30FR membrane, (5) addition of five different antiscalants, (6) temperature 22°C and (7) apparatus in dead-end mode. For the tests using MM a significant decrease in the absolute permeate flux was observed compared with the test without the addition of antiscalants. The chemicals which were supposed to prevent scaling phenomena react with specific components in the water causing an apparent decline in process efficiency. In some

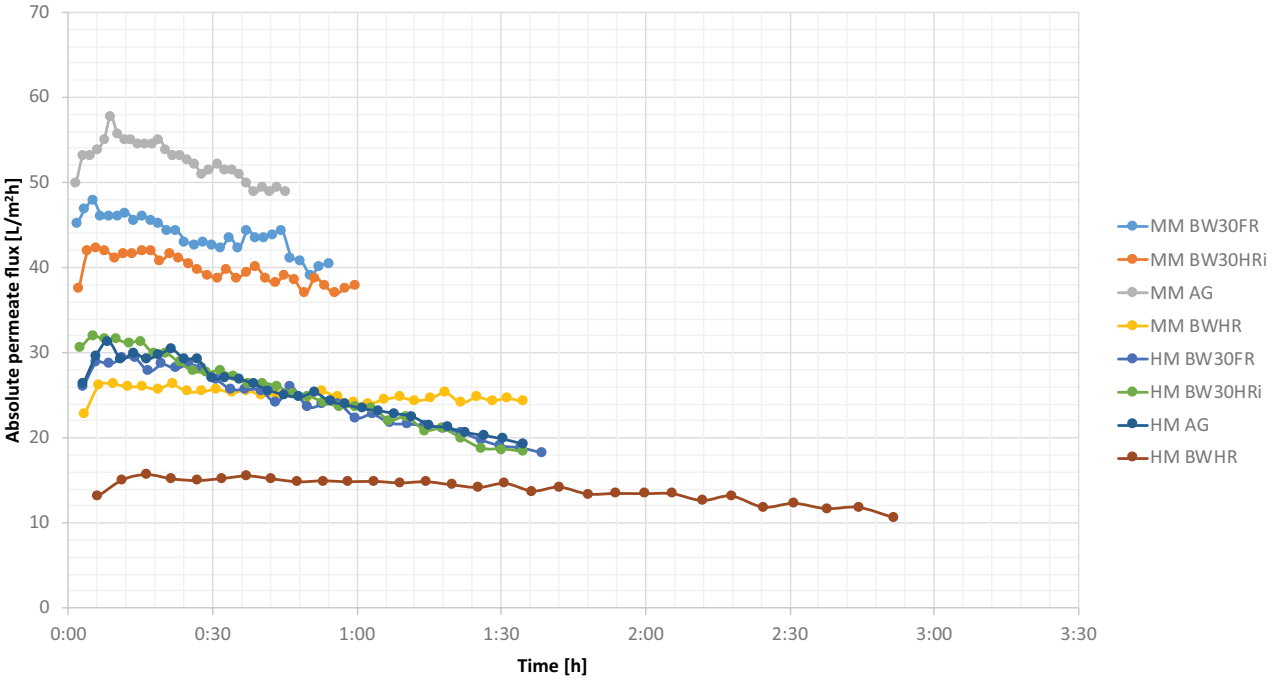

Fig. 8. Comparison changes of permeate flux during reverse osmosis process of medium mineralised and highly mineralised water with four types of reverse osmosis membranes.

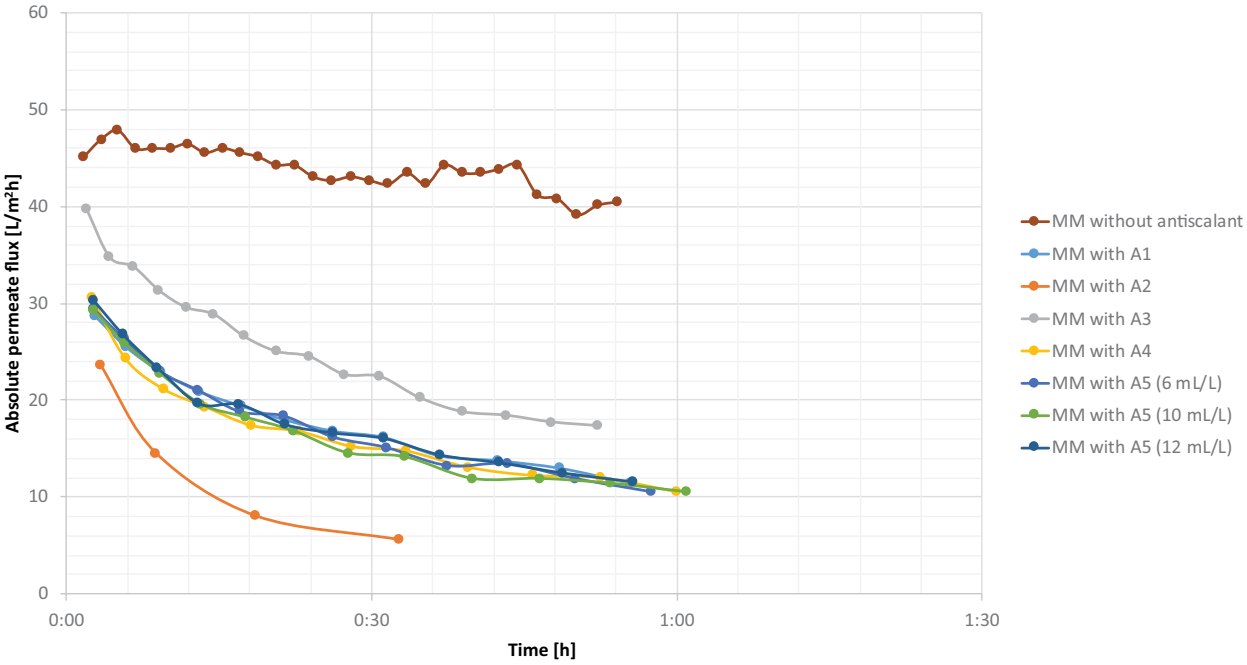

Fig. 9. Comparison changes of permeate flux during reverse osmosis process of medium mineralised water with antiscalants.

cases, the process was discontinued due to a dramatic decline in flux, especially for the process with the addition of the A2 antiscalant. The smallest decrease of absolute permeate flux was gained for the process with the addition of A3 antiscalant, the average permeate flux for this process was 26 L/m²h. The lowest value of average permeate flux was 9 L/m²h for the process with A2 (MM water). For MM the absolute permeate flux changes from 40 L/m²h (for A3) to 6 L/m²h (for A2). For processes with A1, A4 and all doses of A5, the shapes of the curves of absolute permeate flux are similar and present the same trend, values varied from around 30 to 11 L/m²h. Fig. 10 presents the changes of absolute permeate flux with time for the tests using HM water, its values apparently decreasing less than for the

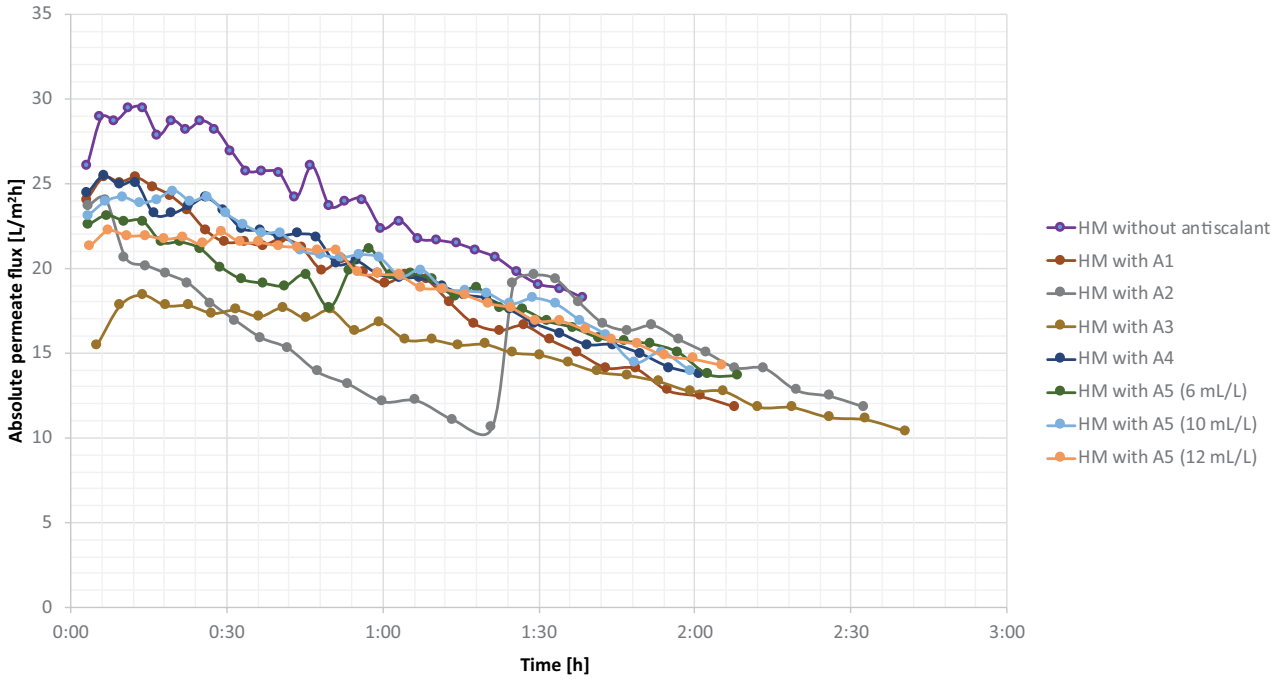

Fig. 10. Comparison changes of permeate flux during reverse osmosis process of highly mineralized water with antiscalants.

processes with MM (from more than 25 L/m²h to around 10 L/m²h). With HM it is hard to determine with which antiscalant the best values were obtained since fewer apparent differences were observed. The highest rates of average permeate flux were obtained with A4 and A5 (10 mL/L), both totalling 20 L/m²h, and for A1 and A5 (6 and 12 mL/L) they were 19 L/m²h. The lowest rates were established for A3 and A2, 15 and 16 L/m²h, respectively. Generally, it can be concluded that addition of antiscalant has aggravated the decrease of absolute permeate flux with time, moreover it has progressed in a harsher manner for MM than for HM. Different doses of A5 caused only minor changes in permeate flux, but did not change the general trend of lowering the permeate flux over time. The sudden increase in the rate of absolute permeate flux for HM (Fig. 10) can be caused by a similar phenomenon to that mentioned in section 3.1, however in this case the increase remains at a higher level.

3.7. Three different feed water temperatures (15°C, 22°C and 30°C)

The influence of feed water temperature was tested with the following process parameters: (1) MM, (2) 50% recovery of permeate, (3) TP 10 bar, (4) NF-LC membrane, (5) temperature 15°C, 22°C and 30°C, and (6) apparatus in cross-flow mode. Fig. 11 presents the experimental data gained from three NF tests with different values of feed water temperature. The results indicated that feed water temperature has a slight influence on unit efficiency. As evidenced, absolute permeate flux changes from 34 L/m²h (for 30°C), 31 L/m²h (for 22°C) and 31 L/m²h (for 15°C) to 31, 28 and 28 L/m²h, respectively. For average permeate flux, the differences were marginal, for tests with feed water temperature established at 15°C and 22°C these values were 29 and 30 L/m²h, for 30°C it was 32 L/m²h. The results from the test with feed water at 30°C indicated that this process was stable over time, which can be seen in the shape of the curve (Fig. 11).

3.8. Three different feed waters (MM, HM and LM)

The influence of water composition on unit efficiency was investigated by applying the following process parameters: (1) MM, HM and LM, (2) 50% recovery of permeate, (3) TP 15 bar, (4) BW30FR membrane, (5) temperature 22°C and (6) apparatus in dead-end mode. The experimental data presented in Fig. 12 indicated that water composition, especially the level of mineralisation, silica and scaling-driven ion concentration, has a direct influence on the absolute value of the permeate flux. As can be seen, it changes from 56 to 50 L/m²h, 48 to 39 L/m²h, and from 29 L/m²h to less than 19 L/m²h, respectively, for LM, MM and HM. The same trend was observed for the lowest temporary average permeate flux values, decreasing from 36 L/m²h for LM, through 28 L/m²h for MM, to 15 L/m²h for HM. The decline is consistent with the mineralisation of the waters used, respectively, less than 0.5, 2.4 and 6.7 g/L (Table 1). However, the high silica content in MM (more than twice that in HM) increases the scaling phenomenon with time which is made evident by a sharp decrease in the curve of absolute permeate flux (Fig. 7). Noteworthy differences are also obtained for average values of permeate flux. The highest value, 53 L/m²h, was obtained for LM, and the lowest for HM (25 L/m²h). For MM, the average permeate flux was established at 44 L/m²h.

3.9. Discussion of the results

Efficiency is an important factor for every action and technology, and also for such a high-energy-demand

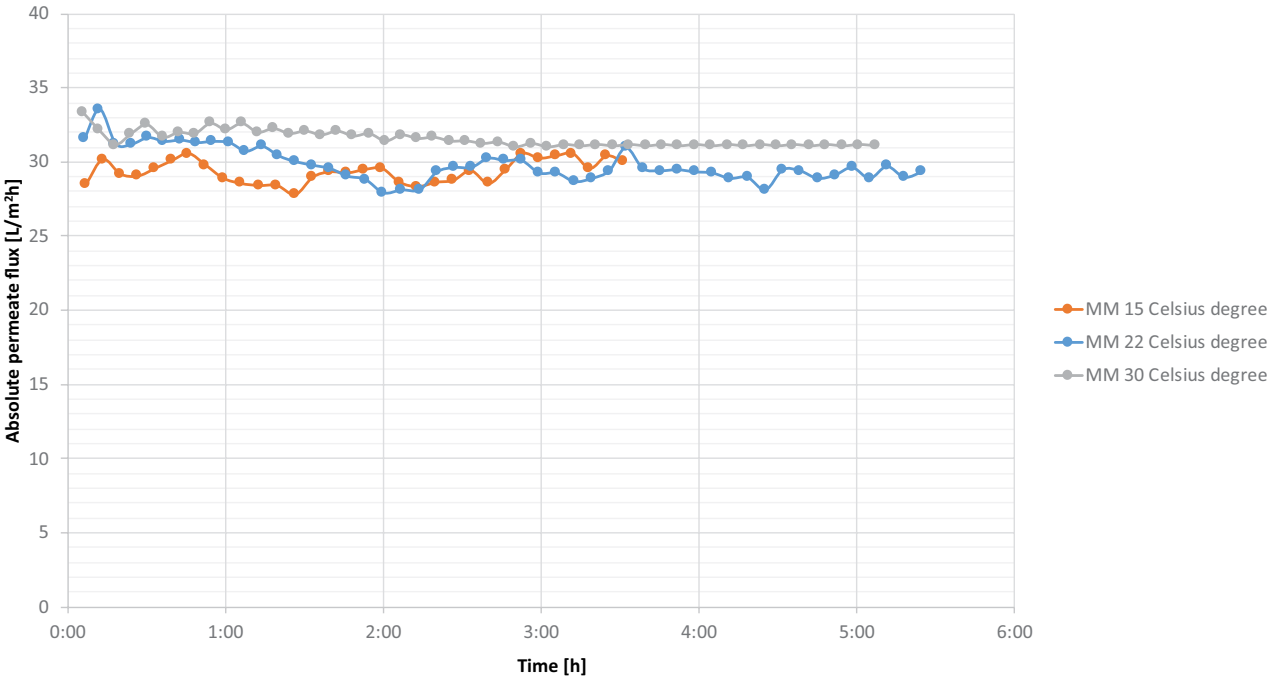

Fig. 11. Comparison changes of absolute permeate flux during NF process of medium mineralised water at different feed water temperatures.

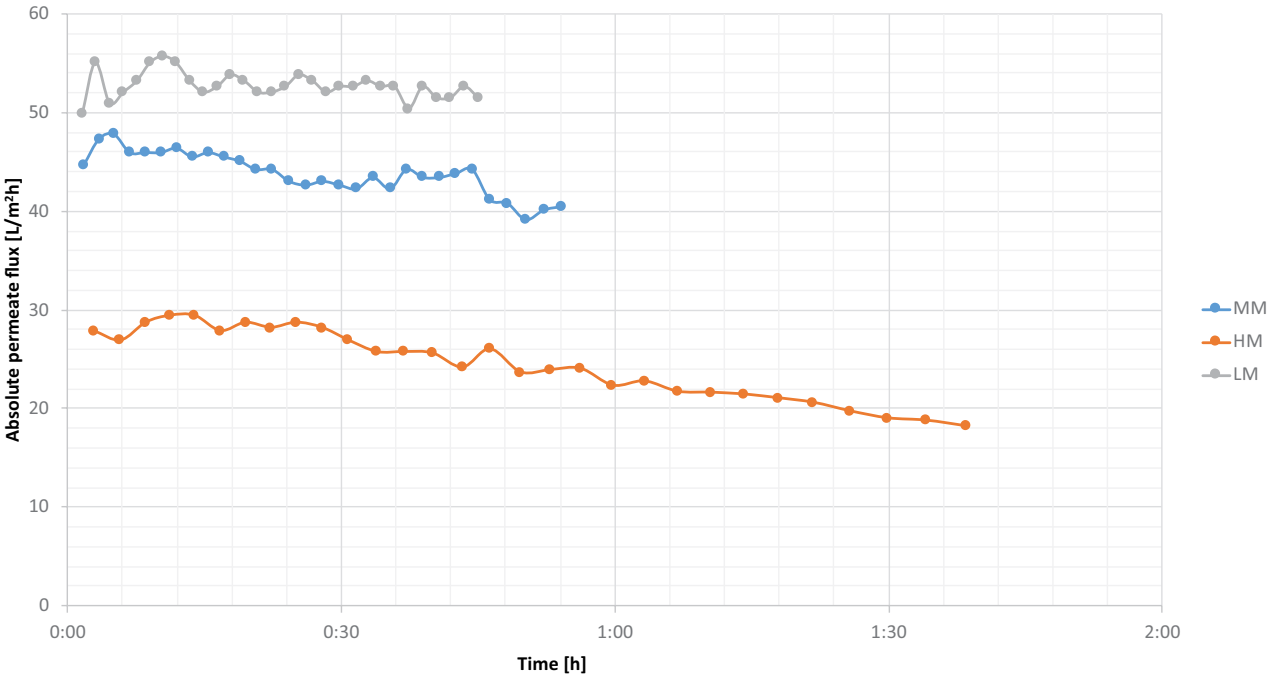

Fig. 12. Comparison changes of absolute permeate flux during RO process of medium mineralised, highly mineralised and lightly mineralised water.

technology as membrane processes, including RO and NF. Energy demand can be successfully assessed by detailed techno-enviro-economic analyses. Adapting the process parameters to the specific composition of geothermal waters can significantly increase the efficiency of the process and thus reduce energy demand. Use of renewable energy sources to fuel the desalination process, including solar and wind energy, can play an important role in the future development of membrane processes in water treatment [45]. In addition, this is important from an ecological point of view, as well as from an economic and energetic one (lowering conventional energy demand).

In the case of membrane technology, it can be stated that it has confirmed its usefulness for clean water production by water concentration or desalination, including using geothermal water [46,47]. This is due to the relatively simple system configuration, its reliability, flexibility and easy integration into hybrid systems [7,10,45]. However, inappropriate values of process parameters, such as permeate recovery, membrane type, feed water temperature, addition of antiscalant, TP, type of apparatus, type of membrane process and water composition, can visibly decrease process efficiency. This was confirmed by the research results presented in this article. For MM (medium-mineralised water), HM (highly mineralised water) and LM (lightly mineralised water), which possess different degrees of mineralisation (2.4 g/L for MM, 6.7 g/L for HM and 0.5 g/L for LM) and concentration of metasilicic acid, it was considered appropriate to indicate the economically and technologically optimal process parameters for further industrial desalination/concentration on the basis of the laboratory tests and analyses presented. All analyses have been directed to significantly increase unit efficiency. Based on the research conducted, the recommended values of process parameters were proposed for the treatment of individual waters (Tables 4 and 5). Considering the type of apparatus used during laboratory tests (cross-flow and dead-end mode), similar parameters to the recommended ones were established for waters with medium and high mineralisation. However, as far as lightly-mineralised water is concerned, the application of a higher value of TP (15 bar) did not cause a visible increase in the rate of permeate flux and it is not proposed as an environmentally, economically and technically reasonable response. Moreover, for all waters the addition of antiscalant led to a significant decrease in unit efficiency. The values of relative and average permeate flux visibly depended on the values of particular process parameters. For water with higher mineralisation, a higher value of permeate recovery and lower TP application caused a significant decrease in permeate flux during the time of operation. This effect was enhanced by the progressive scaling phenomenon. The results presented by Lin and Elimelech [48] confirm the possibility of obtaining greater output efficiency with an appropriate system design and the operation of a RO system, and in addition the tests carried out by Voutchkov [49] indicated that technological advances, including RO system configurations and higher efficiency types of membrane, are projected to further decrease the energy needed.

On the other hand, Chong et al. [50] has made an economic evaluation of energy efficiency for hydrate-based desalination of water. The results presented indicate that innovative hydrate-based desalination utilising liquefied natural gas cold energy can significantly reduce the cost of water due to an appropriate water recovery rate and the adjustment of the plant capacity to its geological location. Saleem and Zaidi [51] underlined that in recent years, scientific studies dedicated to this topic have contributed numerous innovative methodologies. The authors of this publication reviewed the state of the art of RO membrane development, especially the usefulness of nanoparticles in increasing process efficiency. They underlined that nanoparticles demonstrate a pronounced effect in terms of water flux, salt rejection, chlorine resistance, and the anti-fouling properties of thin-film nanocomposite membranes relative to typical thin-film composite membranes. Moreover, they concluded that nanomaterials possess exclusive properties that can contribute to the advancement of high-tech nanocomposite membranes with improved capabilities for desalination. Miladi et al. [52] investigated the energy performance of a solar-powered membrane distillation system. In fact, as far as the solution proposed by the authors is concerned, there is a risk that the efficiency of the process can be unstable and further experimental techno-economic analysis should be carried out. The results presented in this article also showed that proper membrane selection and pressure adjustment significantly increases unit efficiency.

Altmann et al. [53] studied the energy efficiency of the RO process and thermal technologies for water desalination. They underlined that the efficiency of many technologies related to water desalination can be improved by hybridising with other technologies and by leveraging the best aspects of each technology through the adjustment of HM and MM water. The combination of two-stage NF-RO treatment systems for water desalination/concentration can potentially provide the most promising levels of unit efficiency and water purification. However, based on the laboratory tests conducted, the NF process potentially used as a pre-treatment should be conducted with the less-compacted with separation NF membrane (e.g., NF-LC) for MM water and the more-compacted with separation NF membrane for HM water (Fig. 7). For LM water, this solution is not economically justified.

One should agree with the statement that in the case of water desalination, the process parameters used play a key role in the case of energy and process efficiency [54]. This is one of the few issues that the system designer influences from the point of view of obtaining optimal conditions for water desalination [7,11,15,54]. For this reason, the research presented in this article analyses, among other aspects, the effect of selected process parameters and water composition on the efficiency of permeate flux. Energy-efficient desalination and water concentration technologies play a critical role in augmenting freshwater resources and other products (e.g., for the purposes of the cosmetic industry) without placing an excessive strain on limited energy supplies [55,56]. By desalinating high-salinity waters using a rational amount of energy, membrane processes have the potential to increase sustainable water production, a key facet of the water-energy nexus [55,57].

Parallel to the laboratory tests, the authors also carried out experiments using semi-industrial installations with the use of NF-LC and BW30HRi membranes, on the basis of which technological concepts were proposed for MM, HM and LM water desalination/concentration. On the semi-industrial scale, the following process parameters were tested using MM, HM and LM [57]: (1) NF/RO processes, (2) 50%, 75% and other values of permeate recovery, (3) TP 10/15 bar, (4) NF-LC/BW30HRi membranes, (5) temperature 30°C, and different combinations, including two, three or more stages of water desalination/concentration. For MM, a system based on pre-treatment, NF and two stages of RO with two different rates of recovery of permeate, 50% and 75%, was introduced. Similarly, for HM a system based on pre-treatment and two stages of RO with

Table 4
Recommended process parameters and expected absolute permeate flux values for individual waters based on the results of the tests carried out with cross-flow apparatus

Process parameter	MM water	HM water	LM water
Type of membrane process	NF (or NF-RO)	NF (or NF-RO)	NF
Value of permeate recovery (%)	50	50	75
Value of transmembrane pressure (bar)	15	15	10
Membrane type	Less-compacted with separation NF membrane (NF-LC) or less-compacted with separation NF membrane/fouling resistant RO membrane (NF-LC/BW30FR)	More-compacted with separation NF membrane (NF-MC) or less-compacted with separation NF membrane/fouling resistant RO membrane (NF-MC/BW30FR)	Less-compacted with separation NF membrane (NF-LC)
Antiscalant	Without addition	Without addition	Without addition
Feed water temperature (°C)	30	–	–
Expected range of absolute permeate flux for proposed process parameters (L/m^{2}h)	47–29	50–34	25–23
Expected range of average permeate flux for proposed process parameters (L/m^{2}h)	20–31	46–47	21–23

Table 5
Recommended process parameters and expected absolute permeate flux values for individual waters based on the results of the tests carried out with dead-end apparatus

Process parameter	MM water	HM water	LM water
Type of membrane process	RO	RO	RO
Value of permeate recovery (%)	50	50	75
Value of transmembrane pressure (bar)	15	15	10
Membrane type	Fouling-resistant RO membrane (BW30FR)	Fouling-resistant RO membrane (BW30FR)	Fouling-resistant RO membrane (BW30FR)
Antiscalant	Without addition	Without addition	Without addition
Feed water temperature (°C)	–	–	–
Expected range of absolute permeate flux for proposed process parameters (L/m^{2}h)	48–32	29–18	56–39
Expected range of average permeate flux for proposed process parameters (L/m^{2}h)	43–44	23–24	39–53

50% permeate recovery was proposed. However, a system based on pre-treatment and on-stage NF or RO water desalination/concentration was recommended for LM [57]. As can be seen, similar propositions for the particular waters tested were introduced on the basis of the results of tests conducted on a laboratory-scale which are presented in this paper.

In addition to the results for efficiency, the figures presented here indicate that an appropriate selection of process parameters, adapted to water composition, can visibly increase unit efficiency, which directly affects energy and cost demand. The water composition, especially its salinity, directly influences permeate flux and higher values of permeate recovery can become insufficiently effective [5]. Optimising the type of membrane and process (e.g., the NF or RO process) can increase performance with regard to average and absolute permeate flux and reduce operating costs due to the use of lower pressure and reduced process time [22].

4. Conclusions

The efficiency of membrane processes is one of the most important initial considerations in water treatment. There are many parameters, which can have an influence on this matter, in particular: type of membrane process (NF or RO), apparatus type (cross-flow or dead-end mode), value of permeate recovery (e.g., 50% or 75%), TP value (e.g., 15 bar for RO or 10 bar for NF), membrane type (four RO and two NF membranes), addition of antiscalant (five commercially available), feed water temperature (e.g., 22°C, 15°C and 30°C), and chemical composition of the water to be treated (water type). The results of the laboratory study lead us to conclude that to optimise the NF water treatment process, it should be carried out as the main desalination process with a high value of permeate recovery for water with light mineralisation. On the other hand, the RO research showed that in this case the rates of decrease of absolute permeate flux with time that were seen and the addition of antiscalant aggravated the decrease of permeate flux. One can observe the correlation between the process parameters selected and process efficiency. The results also justify the application of antiscalants to visibly decrease the permeate flux with a specific physicochemical composition of the waters such as those tested. Moreover, the experimental data confirm that an appropriate selection of process parameters in accordance with the water's physicochemical composition, especially membrane type, TP value and extent of permeate recovery, may significantly influence the value of absolute and average permeate flux, and consequently the efficiency of the process of concentration of geothermal waters. Moreover, the research indicates that membrane processes can potentially be used as promising technologies with a relatively high efficiency for treatment/concentration of geothermal waters in economic, environmental and technological terms. Recommended values for the process parameters determined from this analysis were proposed for each water (MM, HM and LM) treatment (Tables 4 and 5).

Acknowledgements

This research was partly funded by the Polish National Centre for Research and Development, grant No. 245079 (2014–2017) and Project No. POLTUR 2/1/2017. In addition, this work is part of a doctoral dissertation by Magdalena Tyszer, entitled: Effective and multi-variant use of thermal water concentrates obtained in membrane processes.

References

[1] V.G. Gude, Geothermal source potential for water desalination – current status and future perspective, Renewable Sustainable Energy Rev., 57 (2016) 1038–1065.
[2] B. Tomaszewska, M. Tyszer, Assessment of the influence of temperature and pressure on the prediction of the precipitation of minerals during desalination process, Desalination, 424 (2017) 102–109.
[3] B. Tomaszewska, E. Kmiecik, K. Wątor, M. Tyszer, Use of numerical modelling in the prediction of membrane scaling. Reaction between antiscalants and feedwater, Desalination, 427 (2018) 27–34.
[4] J.A. Sanmartino, M. Khayet, M.C. Garcia-Payo, H. El-Bakouri, A. Riaza, Treatment of reverse osmosis brine by direct contact membrane distillation: chemical pretreatment approach, Desalination, 420 (2017) 79–90.
[5] B.A. Qureshi, S.M. Zubair, Exergetic efficiency of NF, RO and EDR desalination plants, Desalination, 378 (2016) 92–99.
[6] S. Alzahrani, A.W. Mohammad, N. Hilal, P. Abdullah, O. Jaafar, Comparative study of NF and RO membranes in the treatment of produced water II: toxicity removal efficiency, Desalination, 315 (2013) 27–32.
[7] W. Peng, A. Maleki, M.A. Rosen, P. Azarikhah, Optimization of a hybrid system for solar-wind-based water desalination by reverse osmosis: comparison of approaches, Desalination, 442 (2018) 16–31.
[8] A.M. Blanco-Marigorta, A. Lozano-Medina, J.D. Marcos, The exergetic efficiency as a performance evaluation tool in reverse osmosis desalination plants in operation, Desalination, 413 (2017) 19–28.
[9] F.E. Ahmed, R. Hashaikeh, A. Daibat, N. Hilal, Mathematical and optimization modelling in desalination: state-of-the-art and future direction, Desalination, 469 (2019) 114092, https://doi.org/10.1016/j.desal.2019.114092.
[10] J. Duan, Y. Pan, F. Pacheco, E. Litwiller, Z. Lai, I. Pinnau, High-performance polyamide thin-film-nanocomposite reverse osmosis membranes containing hydrophobic zeolitic imidazolate framework-8, J. Membr. Sci., 476 (2015) 303–310.
[11] B.A. Qureshi, S.M. Zubair, Exergetic analysis of a brackish water reverse osmosis desalination unit with various energy recovery systems, Energy, 93 (2015) 256–265.
[12] B.K. Pramanik, Y. Gao, L. Fan, F.A. Roddick, Z. Liu, Antiscaling effect of polyaspartic acid and its derivative for RO membranes used for saline wastewater and brackish water desalination, Desalination, 404 (2017) 224–229.
[13] A. Ruiz-Garcia, J. Feo-Garcia, Estimation of maximum water recovery in RO desalination for different feedwater inorganic compositions, Desal. Water Treat., 70 (2017) 34–45.
[14] J. Nihill, A. Date, P. Lappas, J. Velardo, Investigating the prospects of water desalination using a thermal water pump coupled with reverse osmosis membrane, Desalination, 445 (2018) 256–265.
[15] A. Ruiz-Garcia, I. Nuez, Long-term performance decline in a brackish water reverse osmosis desalination plant. Predictive model for the water permeability coefficient, Desalination, 397 (2016) 101–107.
[16] A. Matin, F. Rahman, H.Z. Shafi, S.M. Zubair, Scaling of reverse osmosis membranes used in water desalination: phenomena, impact, and control; future directions, Desalination, 455 (2019) 135–157.
[17] G.-K. Lu, H. Huang, Dependence of initial silica scaling on the surface physicochemical properties of reverse osmosis membranes during bench-scale brackish water desalination, Water Res., 150 (2019) 358–367.
[18] T. Neveux, M. Bretaud, N. Chim, K. Shakourzadeh, S. Rapenne, Pilot plant experiments and modeling of $CaCO_3$ growth

inhibition by the use of antiscalant polymers in recirculating cooling circuits, Desalination, 397 (2016) 43–52.
[19] A. Ruiz-Garcia, Antiscalant cost and maximum water recovery in reverse osmosis for different inorganic composition of groundwater, Desal. Water Treat., 73 (2017) 46–53.
[20] J.A. Bush, J. Vanneste, T.Y. Cath, Comparison of membrane distillation and high-temperature nanofiltration processes for treatment of silica-saturated water, J. Membr. Sci., 570–571 (2019) 258–269.
[21] M.O. Atallah, M.A. Farahat, M.E. Lofty, T. Senjyu, Operation of conventional and unconventional energy sources to drive a reverse osmosis desalination plant in Sinai Peninsula, Egypt, Renewable Energy, 145 (2020) 141–152.
[22] W.L. Ang, D. Nordin, A.W. Mohammad, A. Benamor, N. Hilal, Effect of membrane performance including fouling on cost optimization in brackish water desalination process, Chem. Eng. Res. Des., 117 (2017) 401–413.
[23] X.H. Hu, J.J. Sun, R.C. Peng, Q. Tang, Y.B. Luo, P. Yu, Novel thin-film composite reverse osmosis membrane with superior water flux using parallel magnetic field induced magnetic multi-walled carbon nanotubes, J. Cleaner Prod., 242 (2020) 118423, https://doi.org/10.1016/j.jclepro.2019.118423.
[24] A. Lilane, D. Saifaoui, S. Hariss, H. Jenkal, M. Chouiekh, Modeling and simulation of the performances of the reverse osmosis membrane, Mater. Today: Proc., 24 (2020) 114–118.
[25] X. Zhang, C. Liu, J. Yang, C.-J. Zhu, L. Zhang, Z.-K. Xu, Nanofiltration membranes with hydrophobic microfiltration substrates for robust structure stability and high water permeation flux, J. Membr. Sci., 593 (2020) 177444, https://doi.org/10.1016/j.memsci.2019.117444.
[26] E. Sahinkaya, S. Tuncman, I. Koc, A.R. Guner, S. Ciftci, A. Aygun, S. Sengul, Performance of a pilot-scale reverse osmosis process for water recovery from biologically-treated textile wastewater, J. Environ. Manage., 249 (2019) 109382, https://doi.org/10.1016/j.jenvman.2019.109382.
[27] A.M. Blanco-Marigorta, A. Lozano-Medina, J.D. Marcos, A critical review of definitions for exergetic efficiency in reverse osmosis desalination plants, Energy, 137 (2017) 752–760.
[28] B. Tomaszewka, M. Bodzek, M. Rajca, M. Tyszer, Geothermal water treatment. Membrane selection for the RO process, Desal. Water Treat., 64 (2017) 292–297.
[29] B. Tomaszewska, M. Rajca, E. Kmiecik, M. Bodzek, W. Bujakowski, M. Tyszer, K. Wator, Process of geothermal water treatment by reverse osmosis. The research with antiscalants, Desal. Water Treat., 74 (2017) 1–10
[30] M. Tyszer, B. Tomaszewska, Pilot study of the impact of geothermal water RO concentrate volume minimization on the possibility of comprehensive further use, Desal. Water Treat., 157 (2019) 250–258.
[31] M. Rajca, M. Bodzek, B. Tomaszewska, M. Tyszer, E. Kmiecik, K. Wątor, Prevention of scaling during the desalination of geothermal water by means of nanofiltration, Desal. Water Treat., 73 (2017) 198–207.
[32] B. Tomaszewska, M. Tyszer, M. Bodzek, M. Rajca, The concept of multi-variant use of geothermal water concentrates, Desal. Water Treat., 128 (2017) 179–186.
[33] B. Tomaszewska, M. Rajca, E. Kmiecik, M. Bodzek, W. Bujakowski, K. Wątor, The influence of selected factors on the effectiveness of pre-treatment of geothermal water during the nanofiltration process, Desalination, 406 (2017) 74–82.
[34] DOW FILMTEC BW30FR-400 High Productivity Fouling Resistant RO Element – Product Information (Form No. 609-00391-0910: https://www.lenntech.com/Data-sheets/Dow-Filmtec-BW30FR-400.pdf).
[35] DOW FILMTEC BW30HR-440i High Productivity, High Rejection Brackish Water RO Element with iLEC™ Technology (Form No. 609-02171-0512): http://www.lenntech.com/Data-sheets/ Dow-Filmtec-BW30HR-440i.pdf).
[36] LEWABRANE®RO B400 HR Membrane, Lanxess Deutschland gmbH BU LPT. Available at: http://lewabrane.com/uploads/tx_lxsmatrix/56922478-eng.pdf).
[37] AG Membrane, GE Power, Water & Process Technologies. Available at: http://www.bmpatel.com/GE-Filters-&-Membrance.pdf.
[38] DOW FILMTEC NF270 Nanofiltration Element for Commercial System – Product Information (Form No. 609-00519-1206. Available at: https://www.lenntech.com/Data-sheets/Dow-Filmtec-NF270-4040.pdf).
[39] DOW FILMTEC NF90 Nanofiltration High Productivity Element – Product Information (Form No. 609-00378-1206. Available at: https://www.lenntech.com/Data-sheets/Dow-Filmtec-NF90-400.pdf).
[40] https://www.worldofchemicals.com/chemicals/chemical-properties/hydrex-4101.html)
[41] https://www.worldofchemicals.com/chemicals/chemical-properties/hydrex-4102.html)
[42] https://www.worldofchemicals.com/chemicals/chemical-properties/hydrex-4104.html)
[43] https://www.worldofchemicals.com/chemicals/chemical-properties/hydrex-4109.html)
[44] https://www.link-chemie.com/de/produkte/wasseraufbereitung/chemkomplex-520-asc.html)
[45] H. Sharon, K.S. Reddy, D. Krithika, L. Philip, Viability assessment of solar distillation for desalination in coastal locations T of Indian sub-continent – thermodynamic, condensate quality and enviro-economic aspects, Sol. Energy, 197 (2020) 84–98.
[46] J. Adrianne, F. Alardin, Thermal and membrane process economics: optimized selection for seawater desalination, Desalination, 153 (2020) 305–311.
[47] A. Farsi, I. Dincer, Development and evaluation of an integrated MED/membrane desalination system, Desalination, 463 (2019) 55–68.
[48] S. Lin, M. Elimelech, Kinetic and energetics trade-off in reverse osmosis desalination with different configurations, Desalination, 401 (2017) 42–52.
[49] N. Voutchkov, Energy use for membrane seawater desalination – current status and trends, Desalination, 431 (2018) 2–14.
[50] Z.R. Chong, T. He, P. Babu, J.-N. Zheng, P. Linga, Economic evaluation of energy efficient hydrate based desalination utilizing cold energy from liquefied natural gas (LNG), Desalination, 463 (2019) 69–80.
[51] H. Saleem, S.J. Zaidi, Nanoparticles in reverse osmosis membranes for desalination: a state of the art review, Desalination, 475 (2020) 114171, https://doi.org/10.1016/j.desal.2019.114171.
[52] R. Miladi, N. Frikha, A. Kheiri, S. Gabsi, Energetic performance analysis of seawater desalination with a solar membrane distillation, Energy Convers. Manage, 185 (2019) 143–154.
[53] T. Altmann, J. Robert, A. Bouma, J. Swaminathan, J.H. Lienhard V, Primary energy and exergy of desalination technologies in a power-water cogeneration scheme, Appl. Energy, 252 (2019) 113319, https://doi.org/10.1016/j.apenergy.2019.113319.
[54] A. Altaee, A. Braytee, G.J. Millar, O. Naji, Energy efficiency of hollow fibre membrane module in the forward osmosis seawater desalination process, J. Membr. Sci., 587 (2019) 117165, https://doi.org/10.1016/j.memsci.2019.06.005.
[55] A. Deshmukh, C. Boo, V. Karanikola, S. Lin, A.P. Straub, T. Tong, D.M. Warsinger, M. Elimelech, Membrane distillation at the water-energy nexus: limits, opportunities, and challenges, Energy Environ. Sci., 11 (2018) 1177.
[56] M.W. Shahzad, M. Burhan, K.C. Ng, A standard primary energy approach for comparing desalination processes, Clean Water, 1 (2019) 1–7.
[57] B. Tomaszewska, Ed., Pozyskanie wód przeznaczonych do spożycia oraz cieczy i substancji balneologicznych w procesie uzdatniania schłodzonych wód geotermalnych. Wyd. IGSMiE PAN, Kraków, 2018.